

Supplementary Information for

Interpretable machine learning-accelerated seed treatment by nanomaterials for environmental stress alleviation

Hengjie Yu^{a,b}, Dan Luo^c, Sam Fong Yau Li^d, Maozhen Qu^{a,b}, Da Liu^{a,b}, Yingchao He^{a,b},
and Fang Cheng^{*a,b}.

^aCollege of Biosystems Engineering and Food Science, Zhejiang University, Hangzhou
310058, China

^bKey Laboratory of Intelligent Equipment and Robotics for Agriculture of Zhejiang
Province, Hangzhou 310058, China

^cDepartment of Biological and Environmental Engineering, Cornell University, Ithaca,
New York 14853, USA

^dDepartment of Chemistry, National University of Singapore, 3 Science Drive 3,
Singapore 117543, Singapore

* Corresponding author, fcheng@zju.edu.cn (Fang Cheng)

This supplementary information file includes:

- Methods S1 to S5
- Figures S1 to S21
- Tables S1 to S6

Methods

Method S1. Determination of root:shoot ratio

The root:shoot ratio was calculated as the following equation:

$$\text{Root:shoot ratio} = \frac{\text{root dry weight}}{\text{stem dry weight} + \text{leaf dry weight}} \times 100\%$$

Method S2. Determination of SRI

The SRI was calculated as the following equation:

$$SRI = \sum_{i=1}^{10} \frac{k_i}{k_i^c}$$

where k_i is the value of the i^{th} endpoint for each treatment, and k_i^c is the value of the i^{th} endpoint for the control. SRI comprehensively considers the relative value of nano-primed and control treatment in ten biological endpoints, and thus the SRI for control is 10.0.

Method S3. Analytical method, instrument parameters, and data acquisition of metabolomics analysis

The samples were separated by Agilent 1290 infinity LC ultra performance liquid chromatography (UHPLC) on a C-18 column (column temperature:40 °C). The flow rate of gradient elution was set at 0.4 ml/min, and the injection volume was 2 μ L. The mobile phase A = 25 mM ammonium acetate and 0.5% formic acid in water and mobile phase B = methanol. The gradient elution procedure was as follows: 5% B in the first 0.5 min, linearly increased to 100% in the next 9.5 min, and maintained at 100% for 2 min; then it was linearly decreased to 5% in 6 s and maintained at 5% in the next 3.9 min. The sample was placed in an automatic sampler at 4 °C during the whole analysis.

Parameter settings of ESI source: Ion Source Gas1 (Gas1) at 60, Ion Source Gas2 (Gas2) at 60, curtain gas at 30, ion source temperature at 600 °C, ion spray voltage floating at \pm 5500 V. The instrument was set to collect data in the m/z range of 60-1000 Da in MS only acquisition, and the accumulation time for TOF MS scan was 0.20 s/spectra. The instrument acquired data over the m/z range 25-1000 Da in auto MS/MS acquisition, and the accumulation time for product ion scan was 0.05 s/spectra. Production scans were acquired using information dependent acquisition with high sensitivity mode selected. The parameters were set as follows: the collision energy at 35 V with \pm 15 eV; declustering potential at \pm 60 V (positive and negative modes); exclude isotopes within 4 Da and candidate ions to monitor per cycle at 10.

Method S4. Line fitting of SHAP main effects and SHAP interactions

The line fitting was based on python language using “scipy.optimize” and “numpy.polyfit” packages. The fitting equations are described as follows:

(1) Piecewise linear fitting for SHAP main effects of the TEM size of nanoparticles (Fig. 4e):

$$y = \begin{cases} 2.00 \times 10^{-1} x - 3.87, & x \leq 21.50 \text{ nm} \\ 1.50 \times 10^{-3} x + 3.90 \times 10^{-1}, & x > 21.50 \text{ nm} \end{cases}$$

where x is the TEM size of nanoparticles, and y is the SHAP main effect value.

(2) Linear fitting for SHAP main effects of the zeta potential of nanoparticles (Fig. 4f):

$$y = -1.14 \times 10^{-2} x - 2.77 \times 10^{-2} x$$

where x is the zeta potential of nanoparticles, and y is the SHAP main effect value.

(3) Logistic fitting for SHAP interactions between the zeta potential and concentration of nanoparticles (Fig. 4k):

$$y = \begin{cases} \frac{-2.28}{1 + e^{4.66 + 5.48 \times 10^{-1} x_1}} + 8.39 \times 10^{-1}, & x_2 = 100 \text{ mg/L} \\ \frac{2.29}{1 + e^{10.57 + 9.32 \times 10^{-1} x_1}} - 6.91 \times 10^{-1}, & x_2 = 50 \text{ mg/L} \end{cases}$$

where x_1 is the zeta potential of nanoparticles, x_2 is the concentration of nanoparticles, and y is the SHAP interaction value.

(4) Plateau fitting for SHAP interactions between the TEM size and concentration of nanoparticles (Fig. 4l):

$$y = \frac{-3.96x}{8.51 + x_1} + 3.00, \quad x_2 = 100 \text{ mg/L or } x_2 = 50 \text{ mg/L}$$

where x_1 is the TEM size of nanoparticles, x_2 is the concentration of

nanoparticles, and y is SHAP interaction value.

(5) Polynomial fitting for SHAP main effects of the TEM size of nanoparticles (Fig.

5e):

$$y = 1.66 \times 10^{-6} x^3 - 3.63 \times 10^{-4} x^2 + 2.44 \times 10^{-2} x - 4.27 \times 10^{-1}$$

where x is the TEM size of nanoparticles, and y is the SHAP main effect value.

(6) Polynomial fitting for SHAP main effects of the zeta potential of nanoparticles (Fig.

5f):

$$y = -5.71 \times 10^{-6} x^3 + 2.49 \times 10^{-4} x^2 + 1.89 \times 10^{-3} x - 8.44 \times 10^{-2}$$

where x is the zeta potential of nanoparticles, and y is the SHAP main effect value.

Method S5. Cost estimate of seed nanoprimer (nanoparticles)

Given the following conditions:

ZnO nanoparticle price (30nm, Macklin): RMB ¥ 308 (500 g)

Seed weight: nanoparticle volume: 1:5 g/mL

Planting seeds = 22 kg/ha

Nanoparticle concentration: 200 mg/L

so, we can estimate the nanoparticle fee.

Nanosuspension volume = 22 kg/ha × 5 L/kg = 110 L/ha

Nanoparticle weight = 110 L/ha × 200 mg/L = 22000 mg/ha = 22 g/ha

Nanoparticle fee = 22 g/ha × ¥ 308 ÷ 500 g = ¥ 13.552/ha (around \$ 2/ha)

Figures

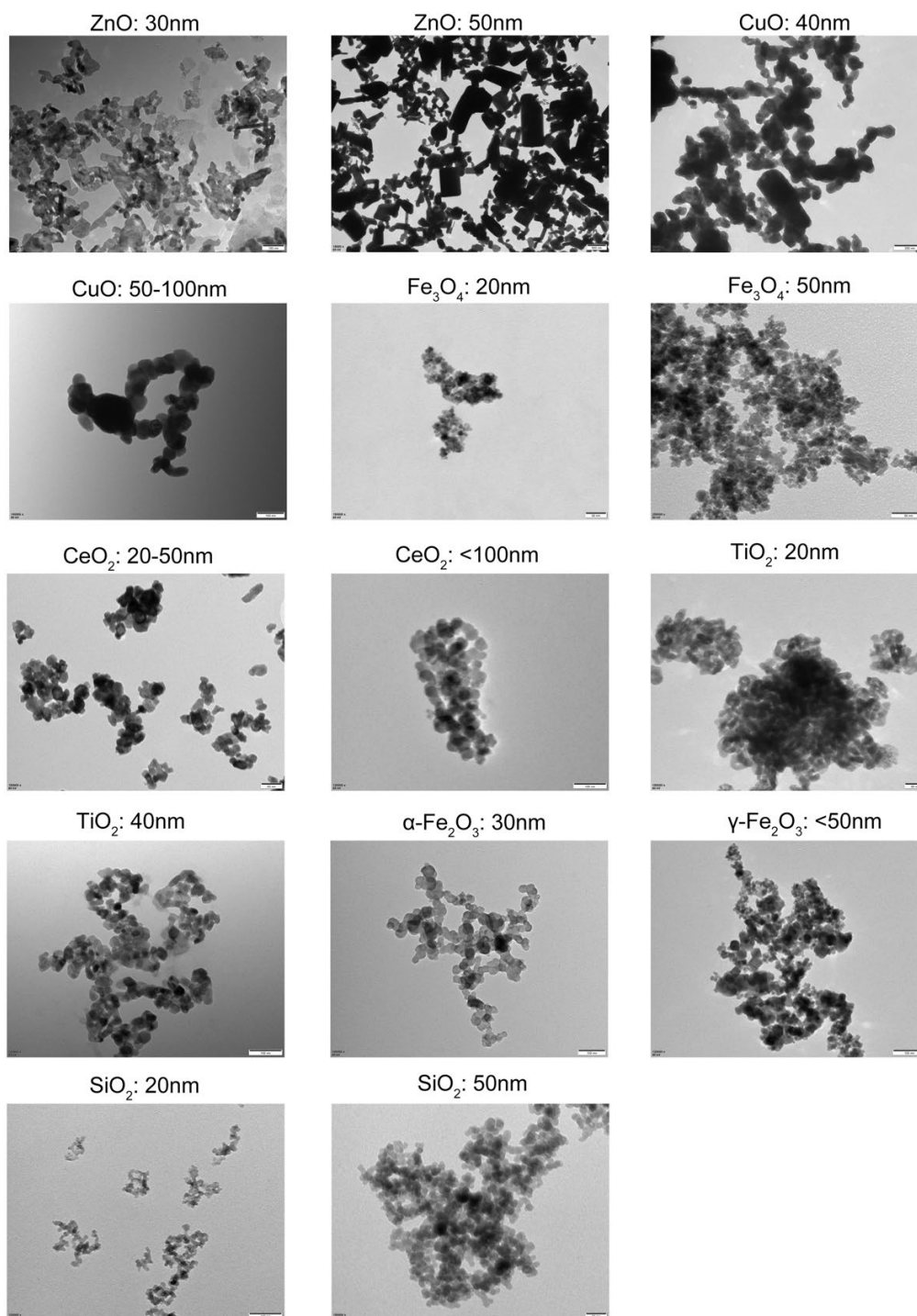


Fig. S1: TEM images of fourteen low-cost metalloid and metal oxide nanoparticles (SiO₂, CeO₂, CuO, Fe₃O₄, ZnO, α-Fe₂O₃, and γ-Fe₂O₃ of different sizes).

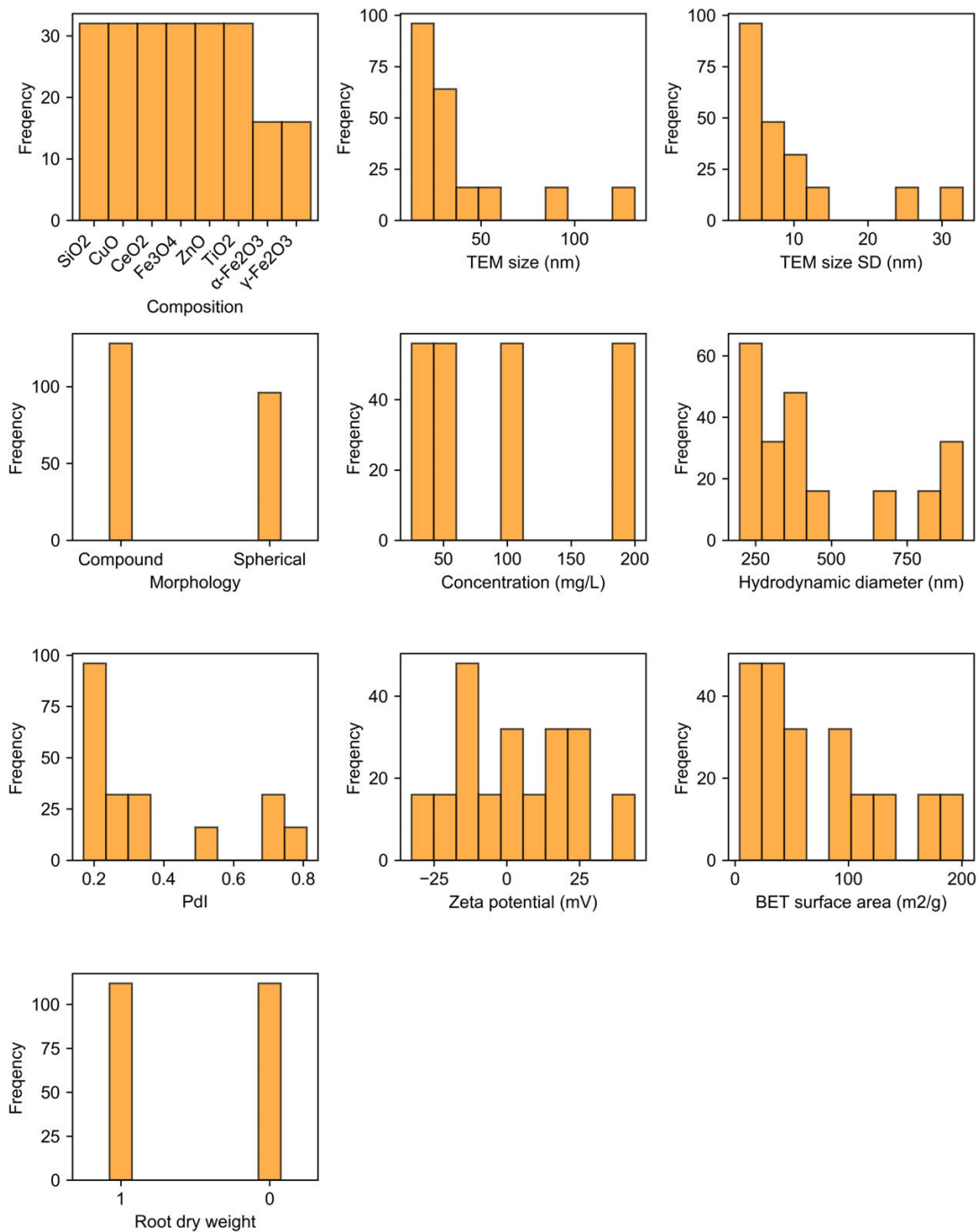


Fig. S2. An overview of the used features and the prediction target (root dry weight).

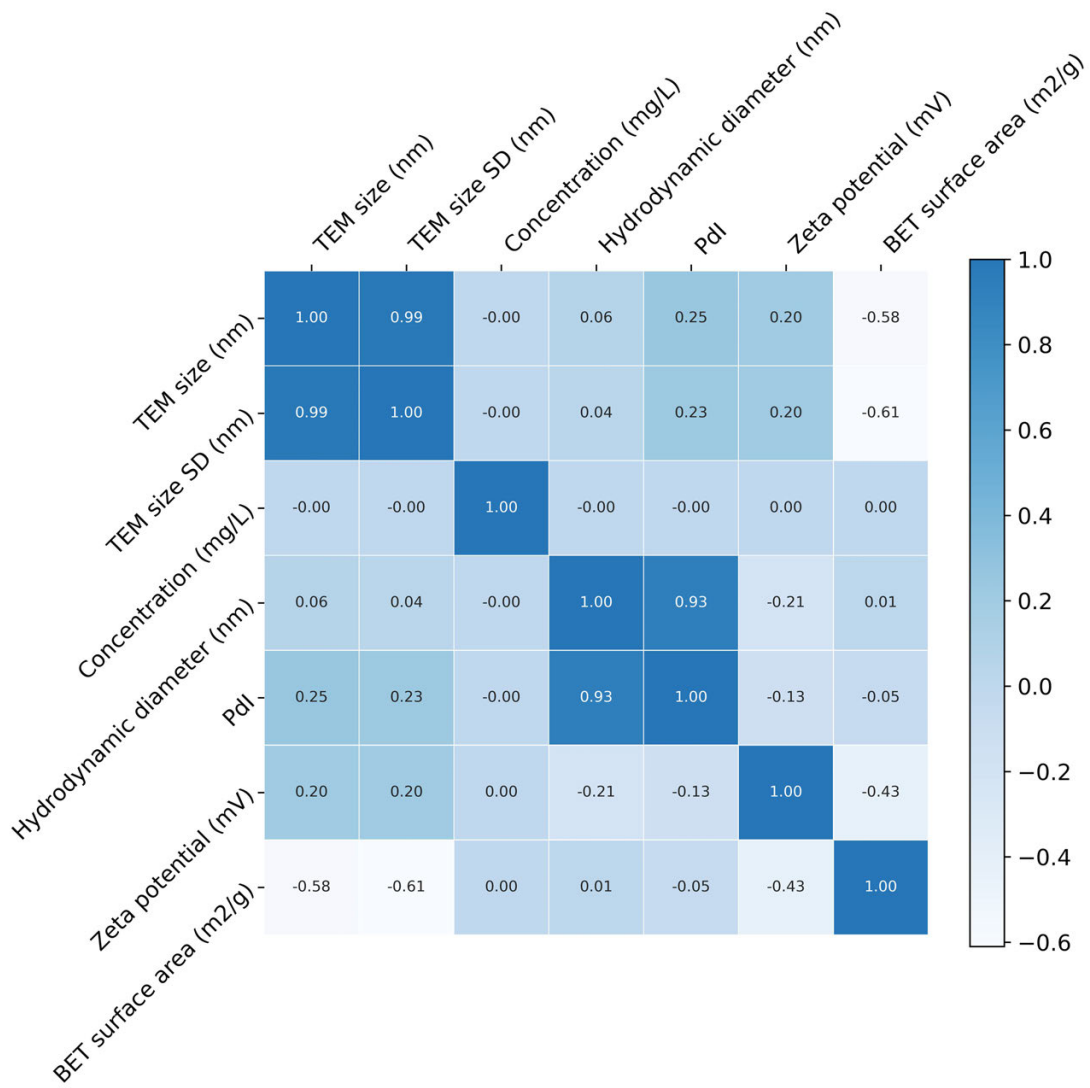


Fig. S3. The heatmap of the Pearson correlation coefficient among numerical factors.

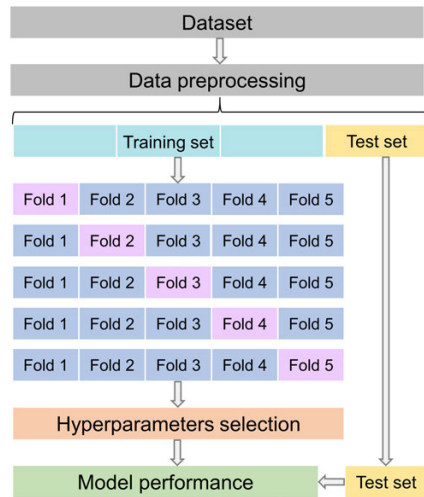


Fig. S4. The workflow for the establishment of the LightGBM models.

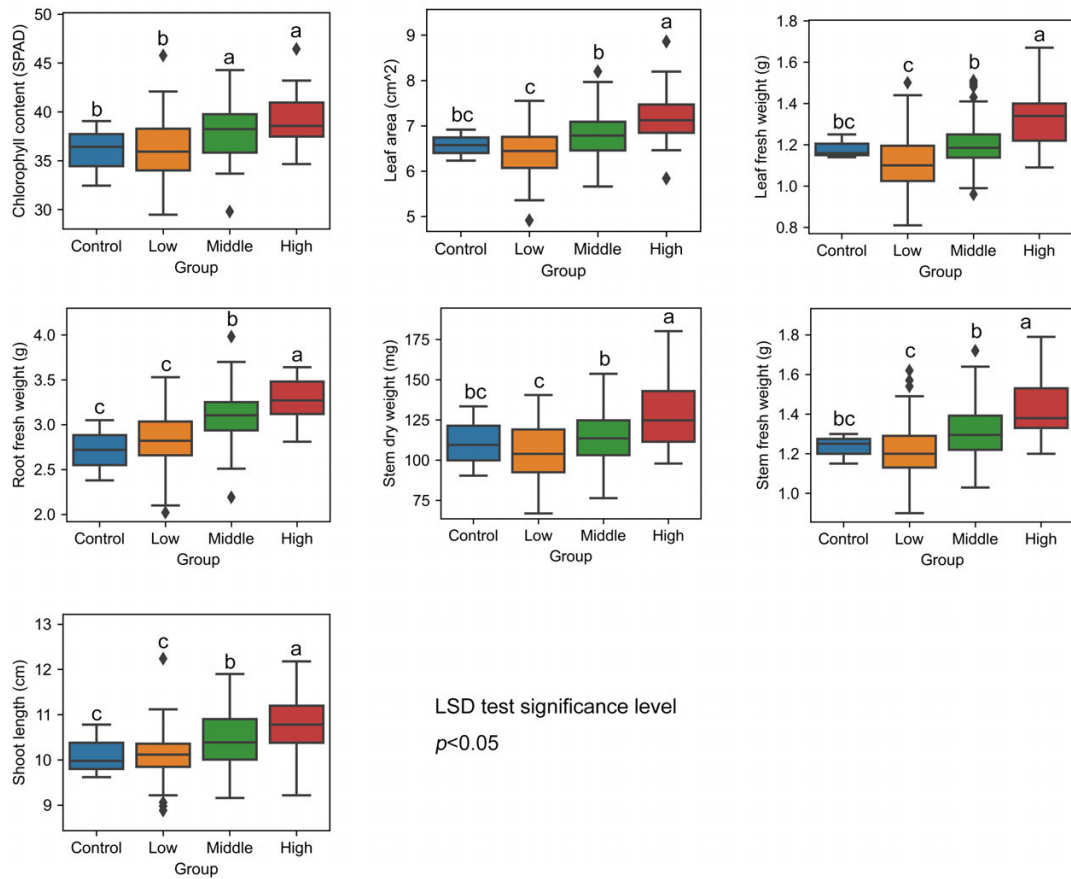


Fig. S5. The differences between three nanopriming groups and the control on biological endpoints under salinity stress.

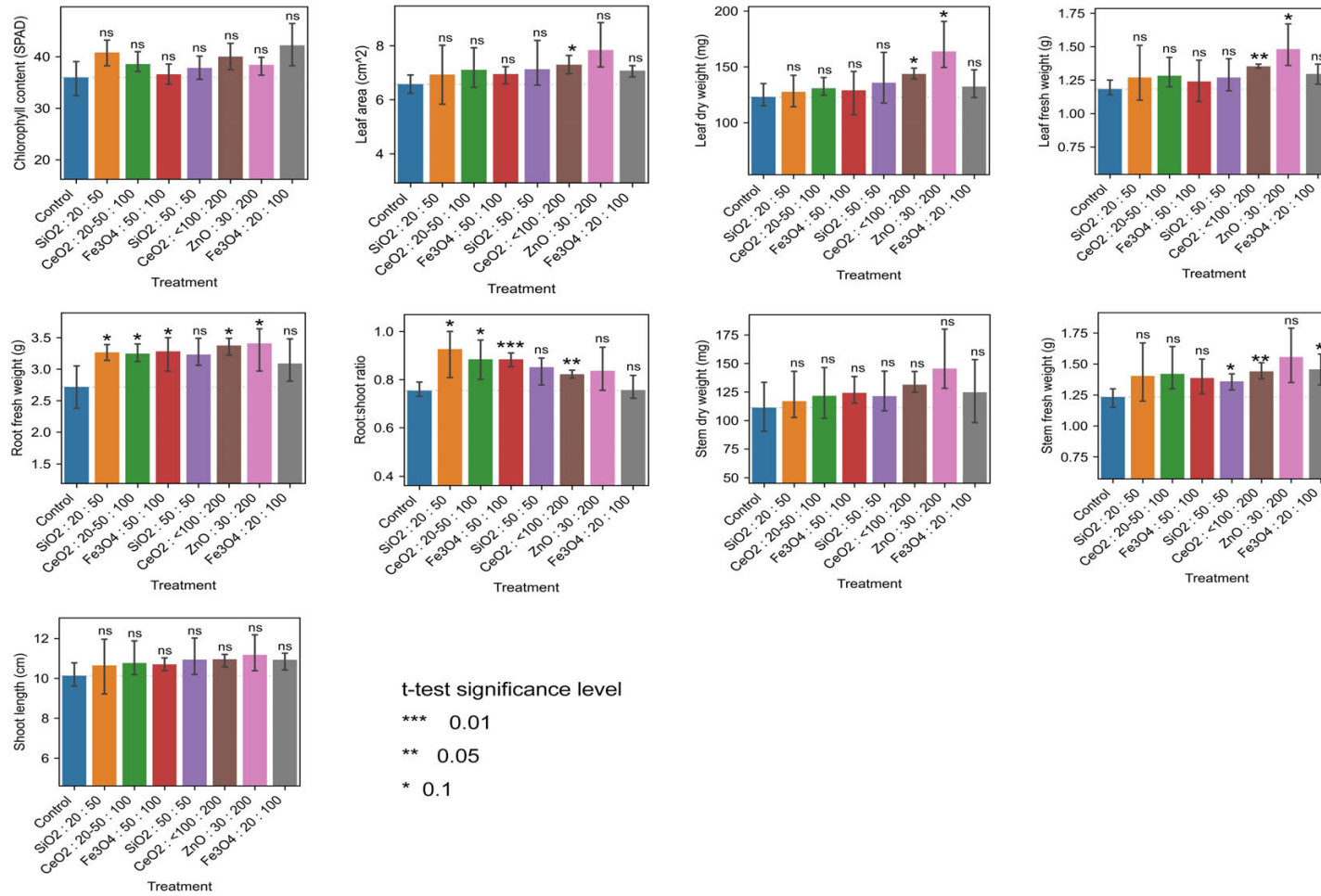


Fig. S6. The comparison of biological endpoints among seven treatments in the High group under salinity stress.

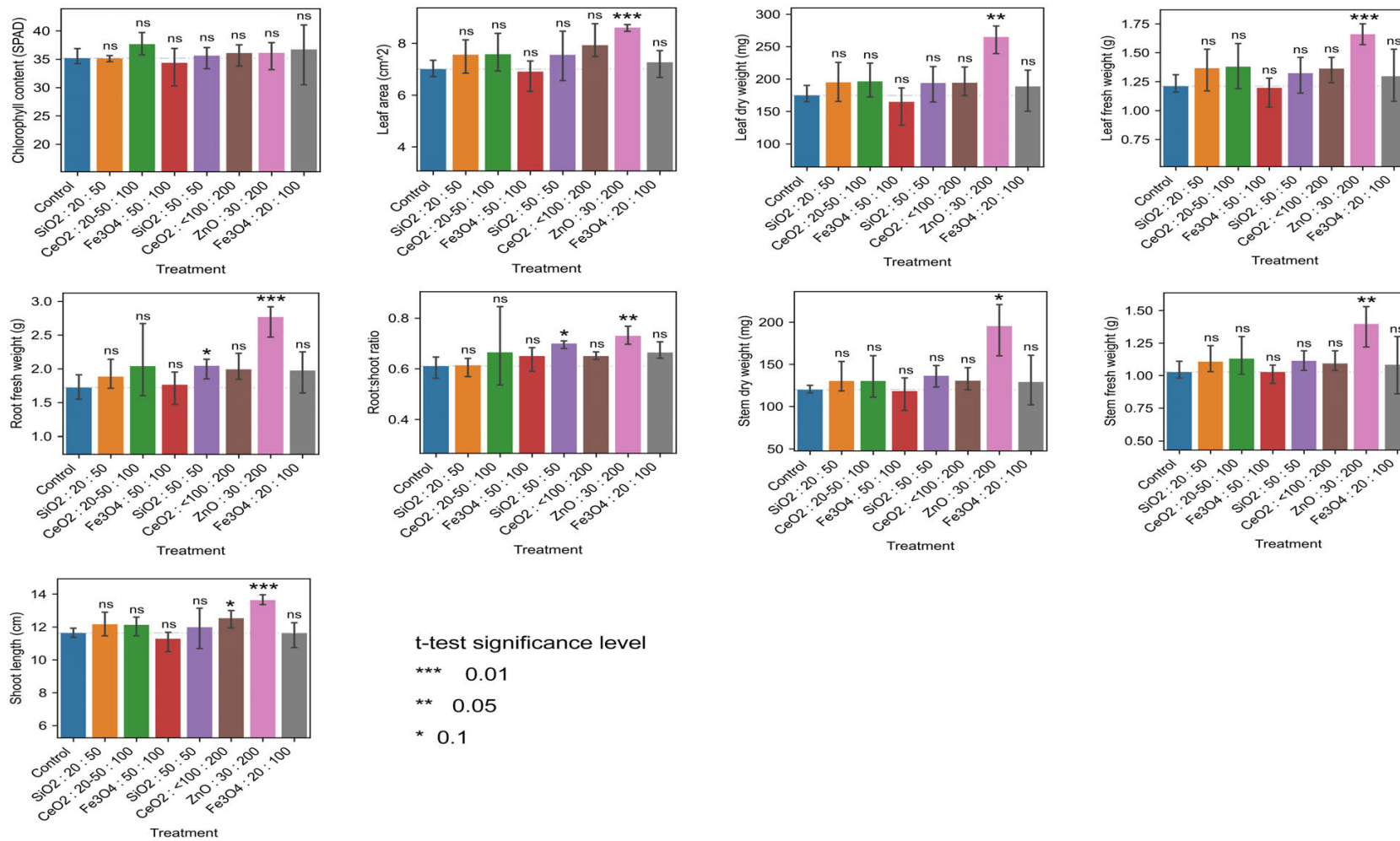


Fig. S7. The comparison of biological endpoints among selected treatments under combined heat-drought stress.

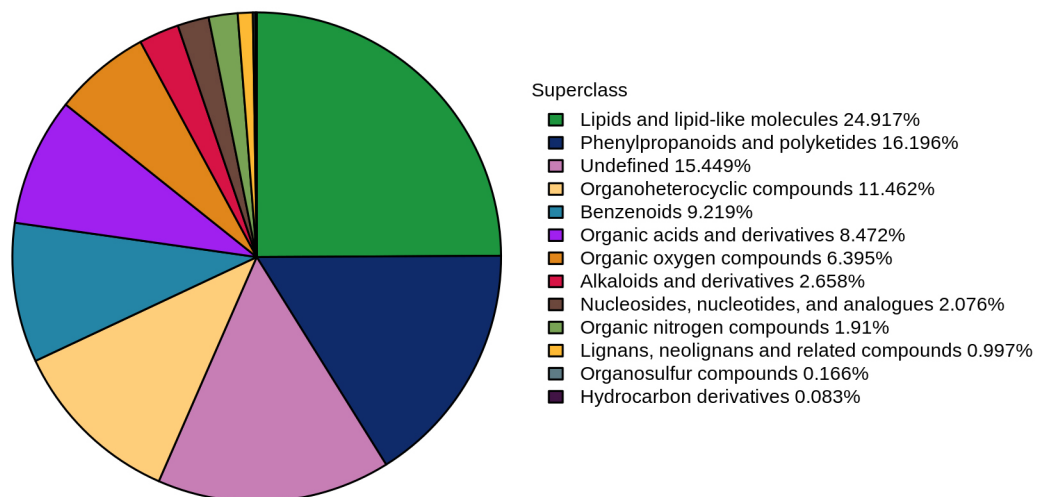


Fig. S8. The superclass of 1204 identified metabolites.

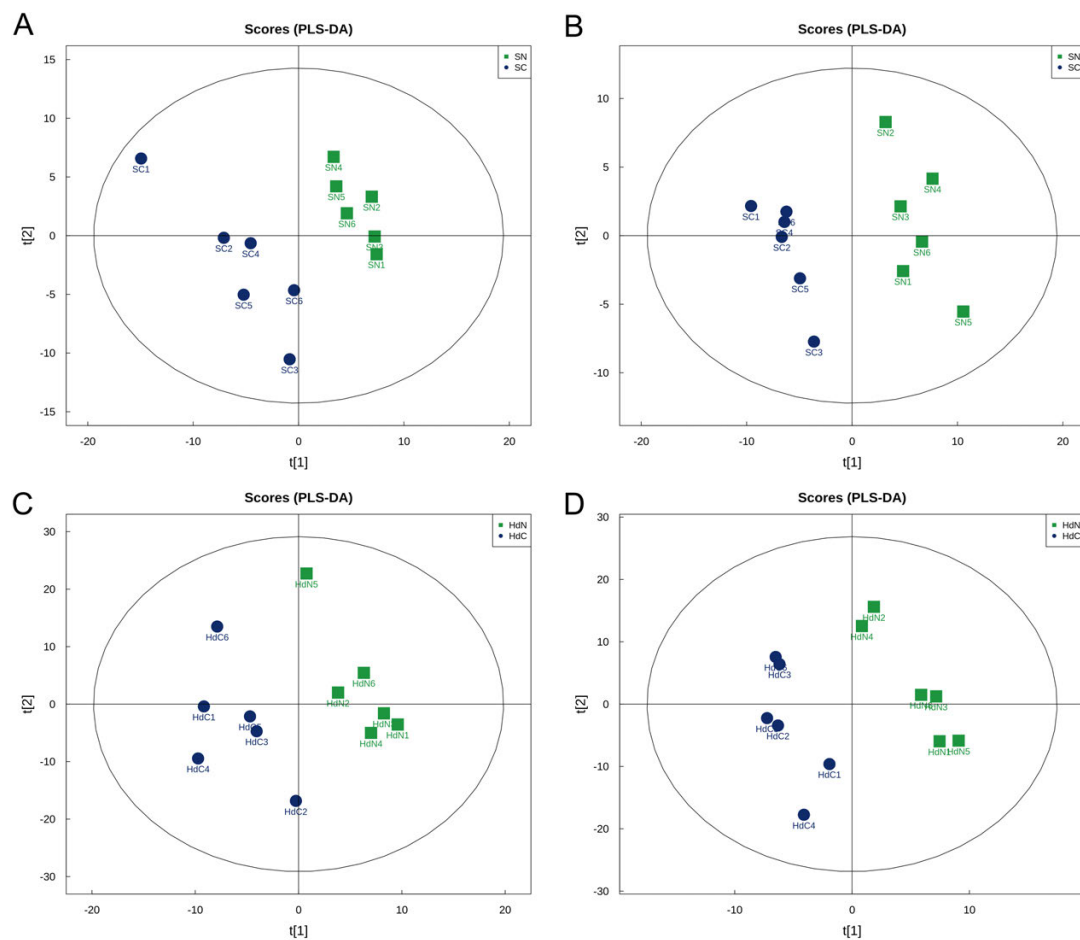


Fig. S9. The score plots of PLS-DA of metabolic profiles in maize leaves after SN and SC seed priming in the positive (A) and negative (B) ion modes. The score plots of PLS-DA of metabolic profiles in maize leaves after HdN and HdC seed priming in the positive (C) and negative (D) ion modes.

A

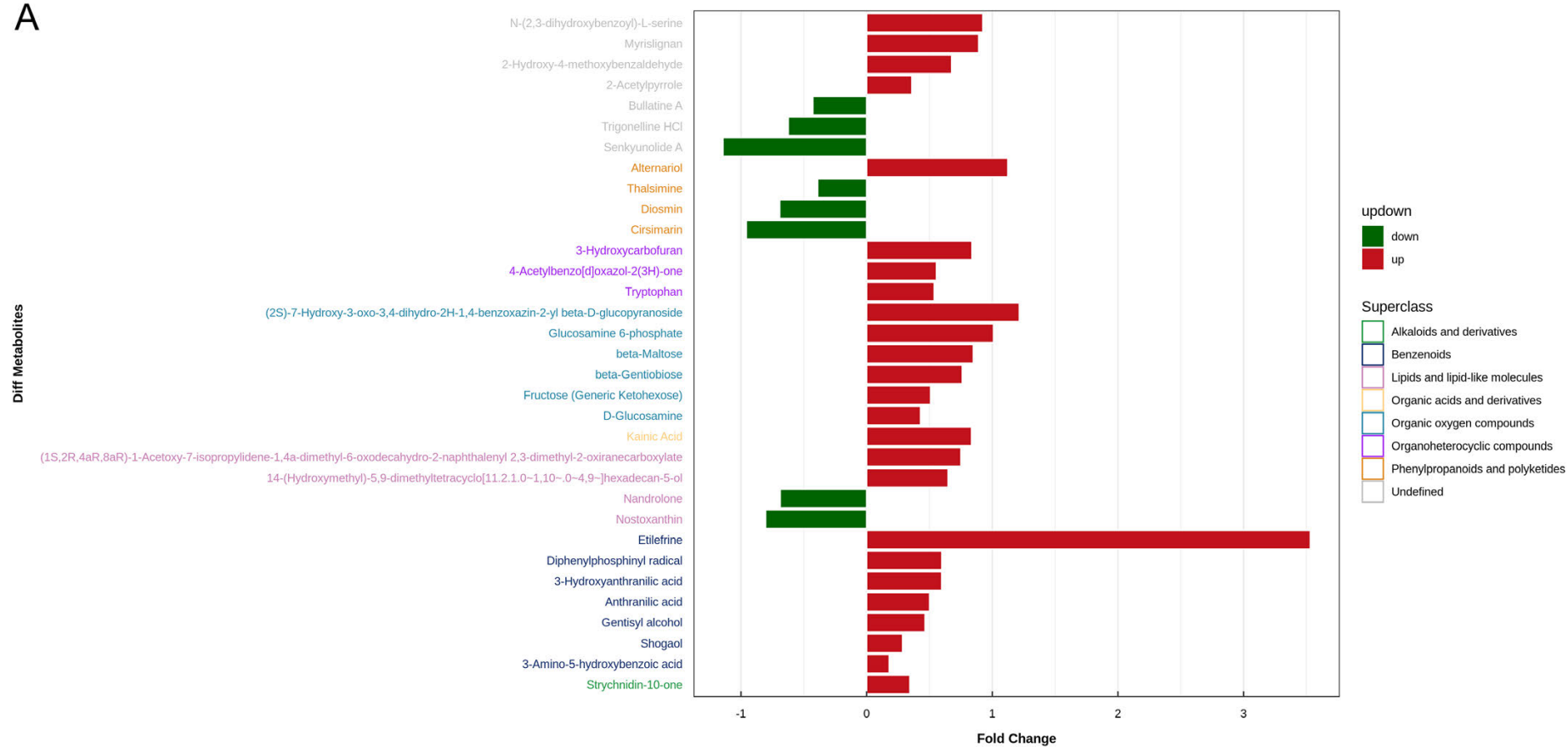


Fig. S10 (A). The up-regulated and down-regulated metabolites in maize leaves after SN and SC seed priming in the positive ion modes.

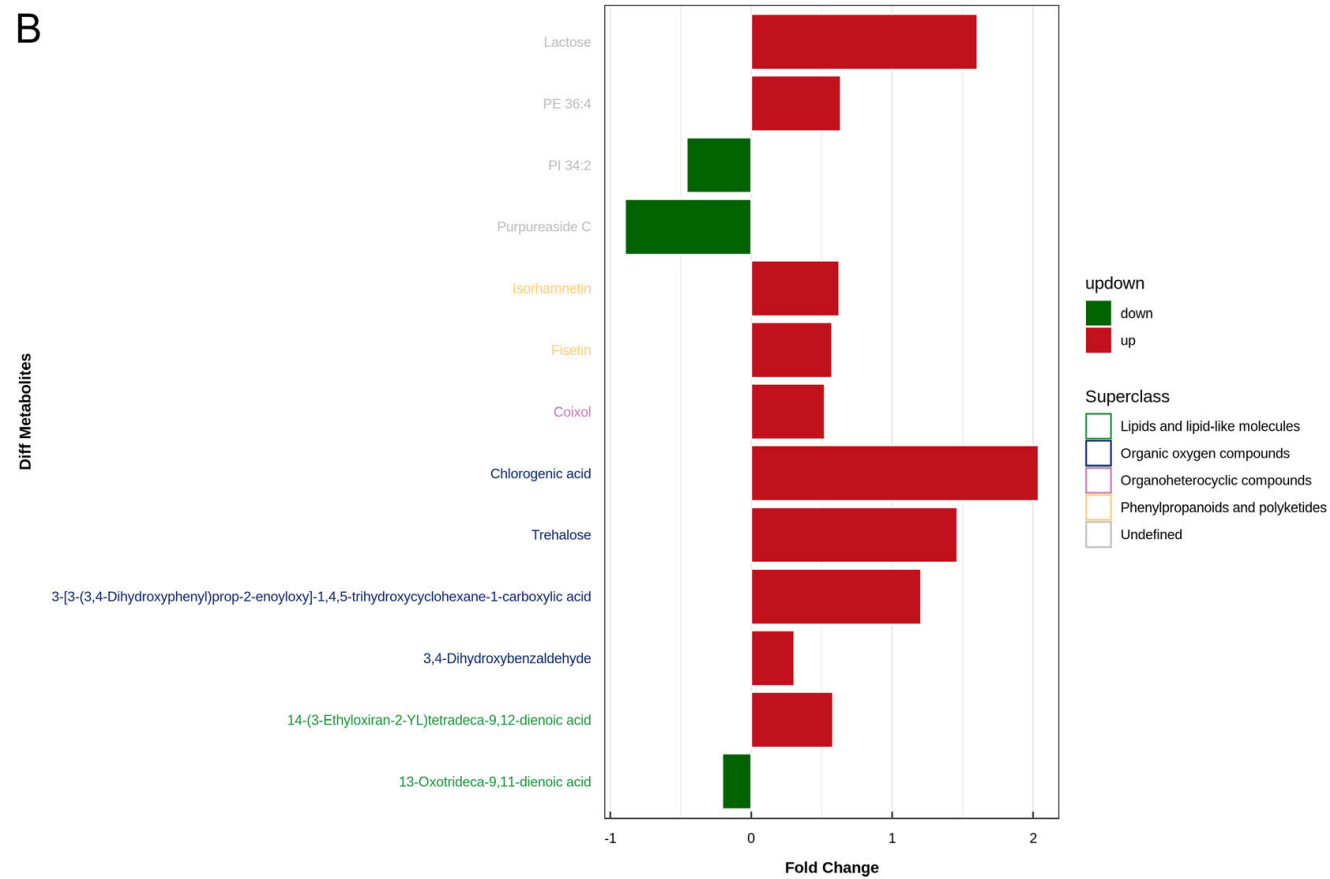


Fig. S10 (B). The up-regulated and down-regulated metabolites in maize leaves after SN and SC seed priming in the negative ion modes.

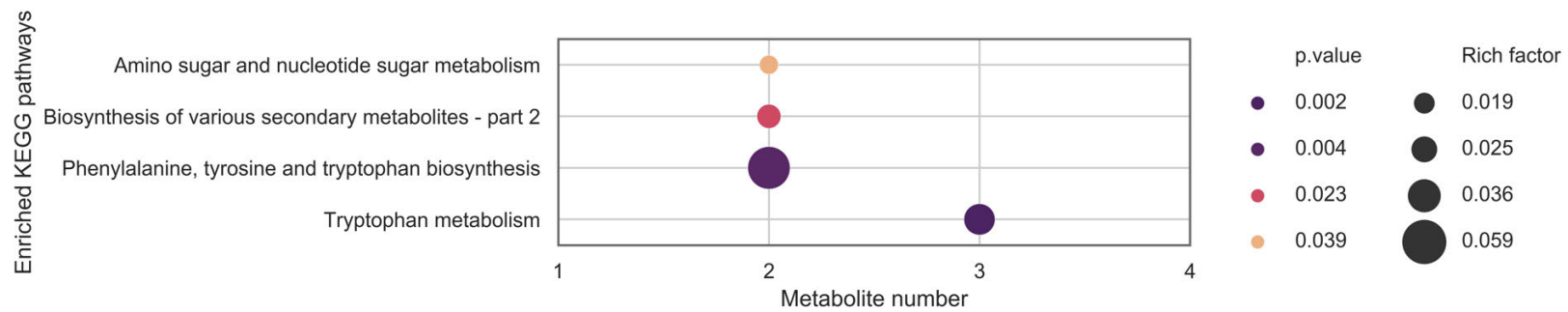


Fig. S11. KEGG pathway enrichment analysis based on significantly different metabolites between SN and SC.

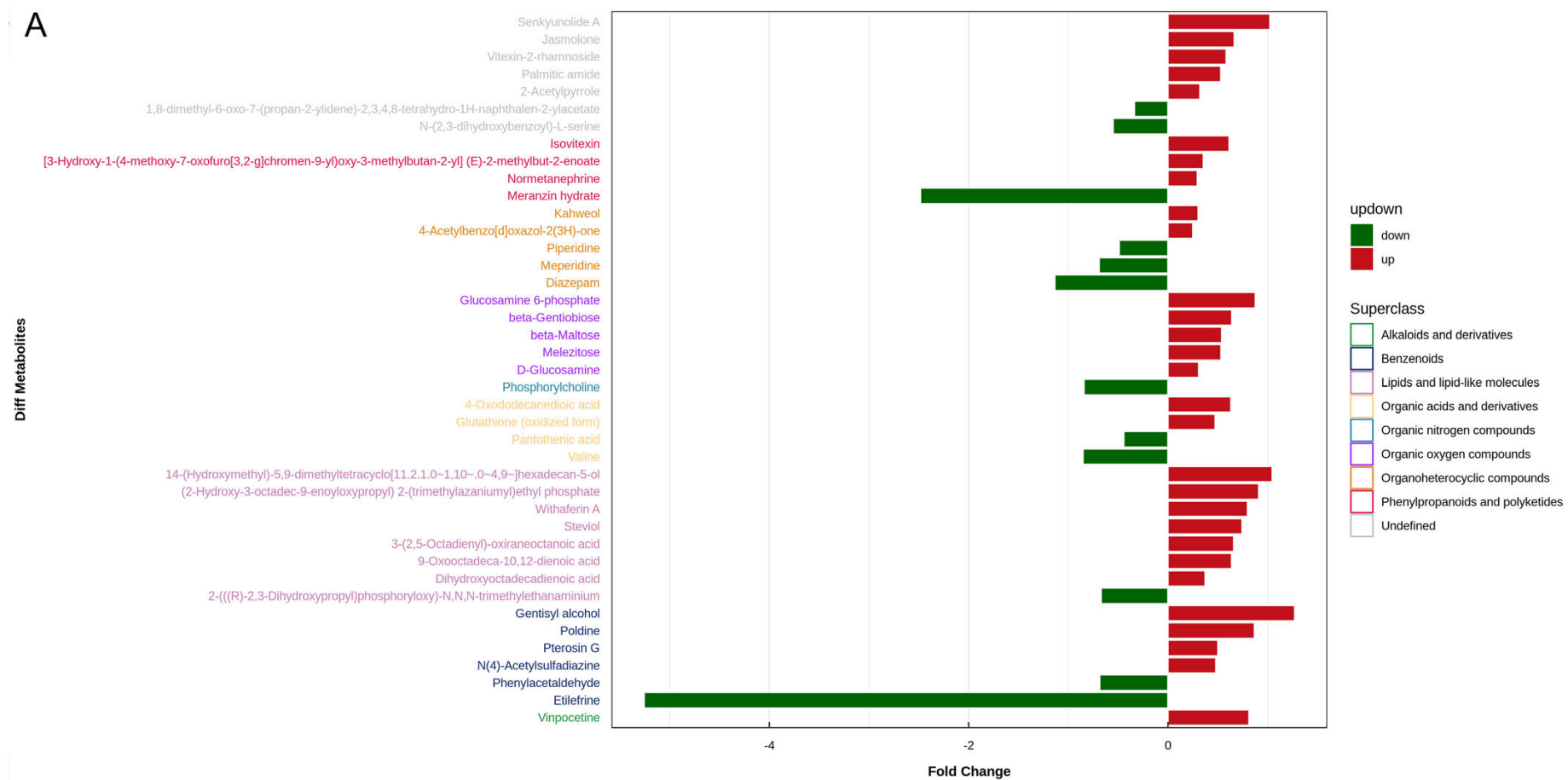


Fig. S12 (A). The up-regulated and down-regulated metabolites in maize leaves after HdN and HdC seed priming in the positive ion modes.

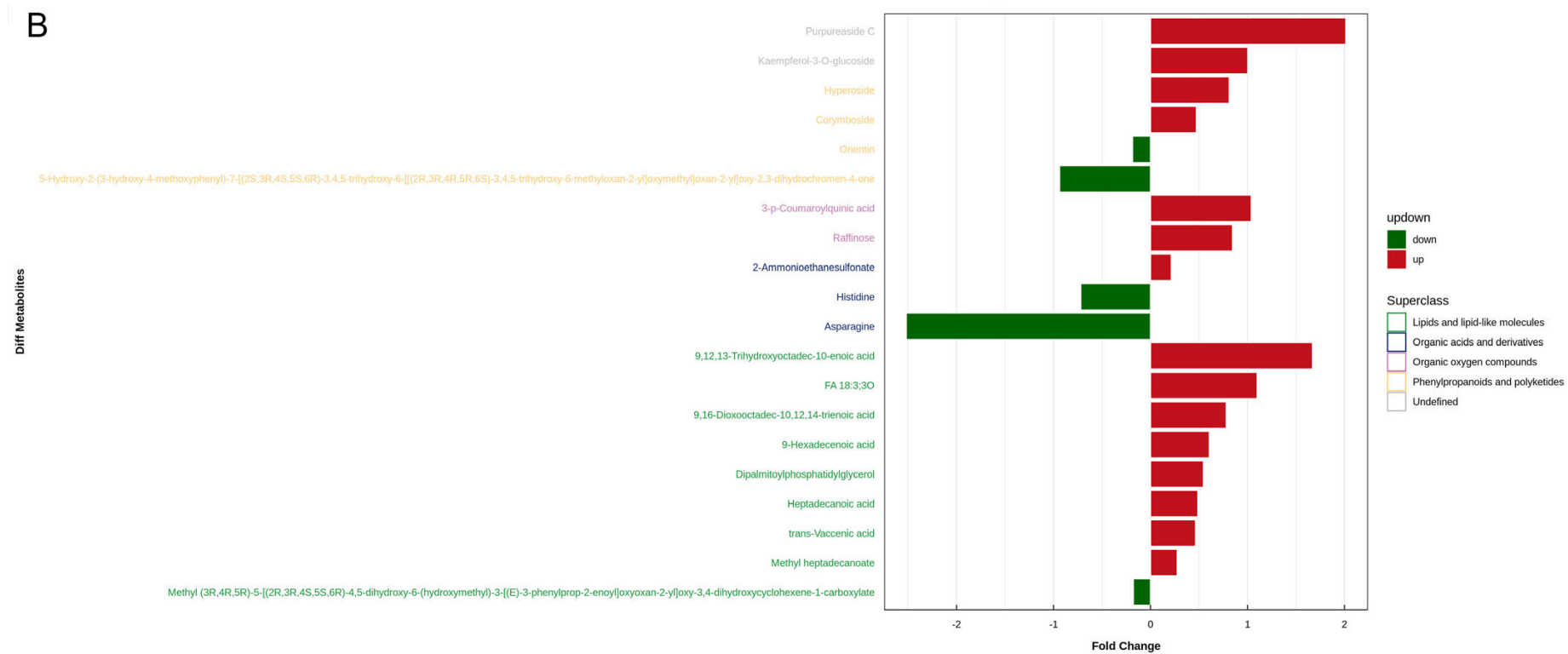


Fig. S12 (B). The up-regulated and down-regulated metabolites in maize leaves after HdN and HdC seed priming in the negative ion modes.

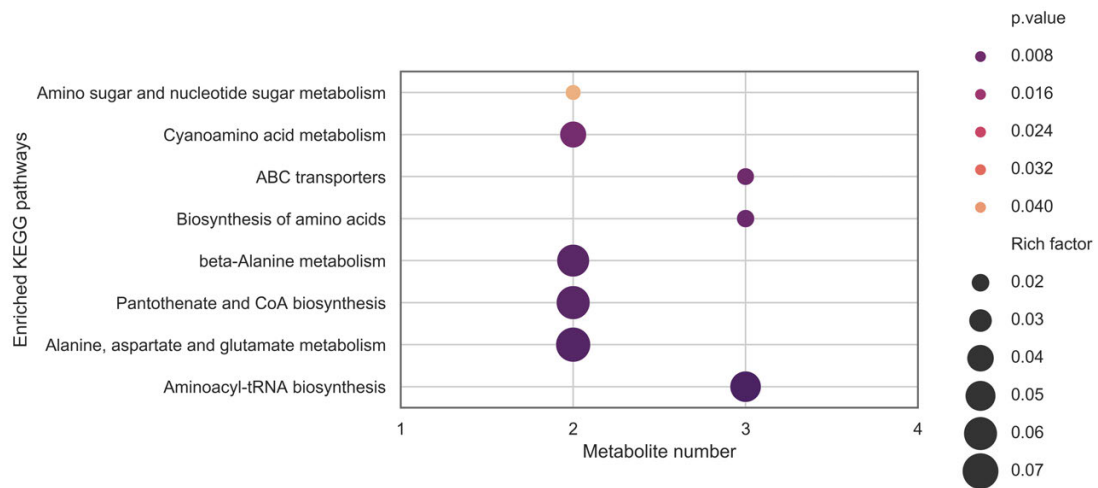


Fig. S13. KEGG pathway enrichment analysis based on significantly different metabolites between HdN and HdC.

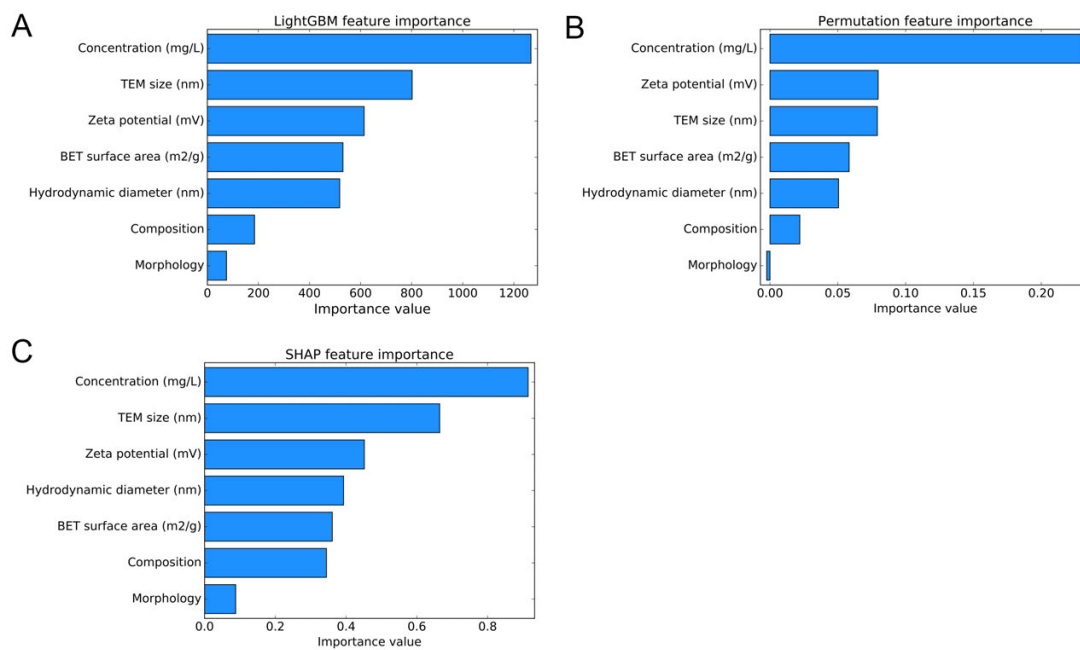


Fig. S14. The absolute values of feature importance obtained by LightGBM feature importance (A), permutation feature importance (B), and SHAP feature importance (C).

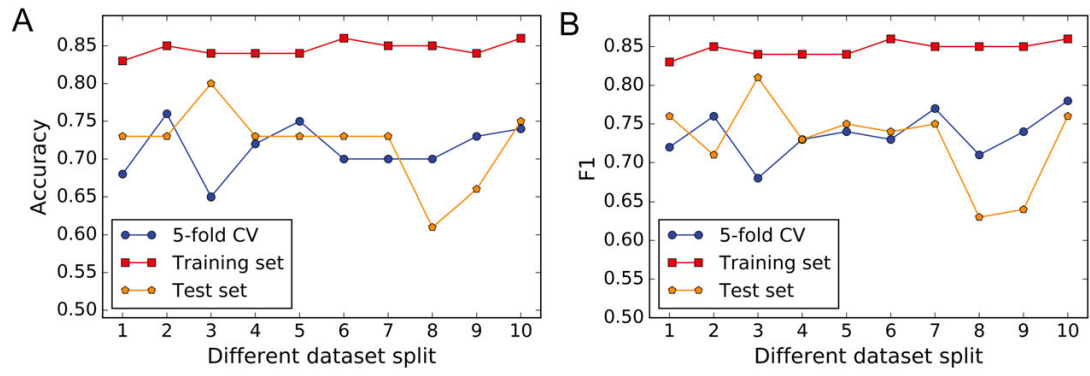


Fig. S15. The accuracy (A) and F1 score (B) of established models on ten dataset splits.

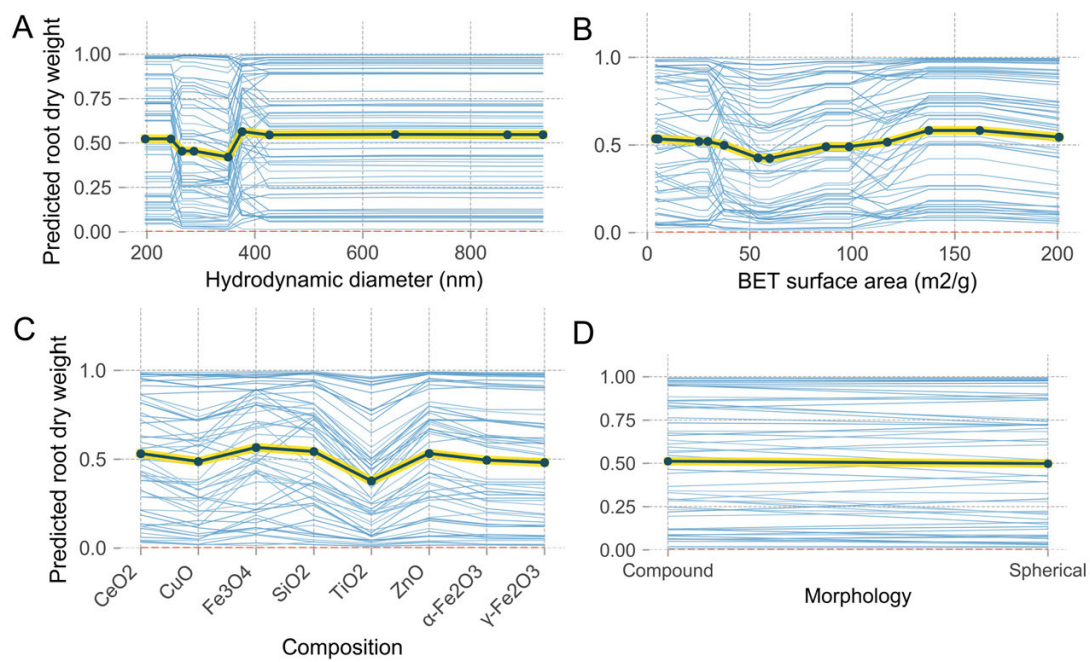


Fig. S16. PDP and ICE plots of hydrodynamic diameter (A), BET surface area (B), composition (C), and morphology (D).

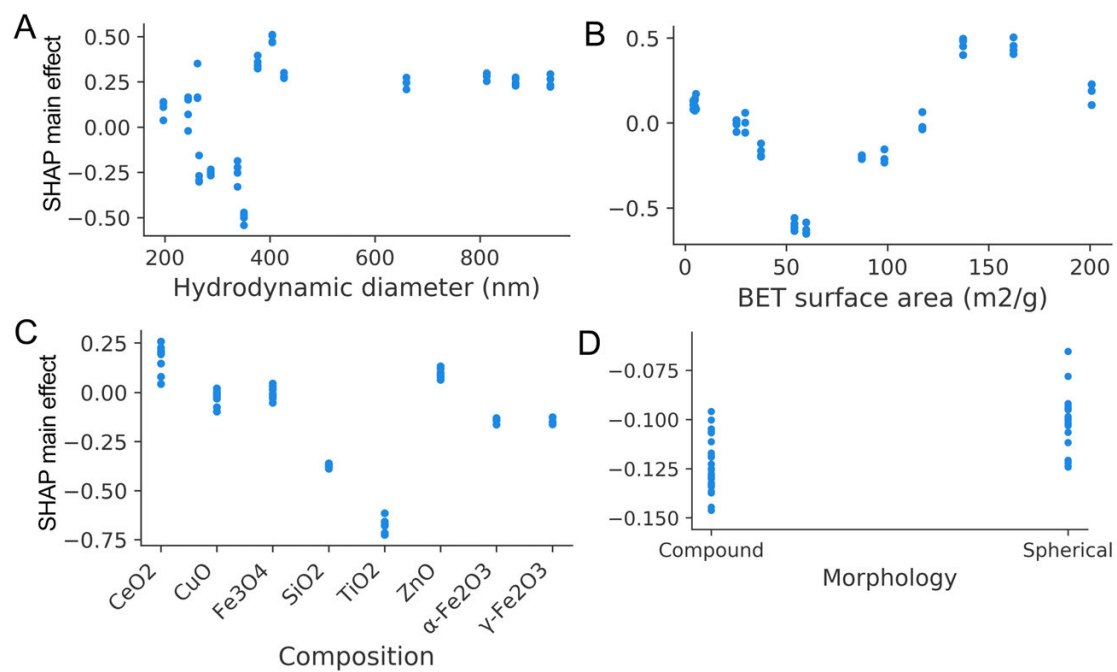


Fig. S17. SHAP main effects of hydrodynamic diameter (A), BET surface area (B), composition (C), and morphology (D).

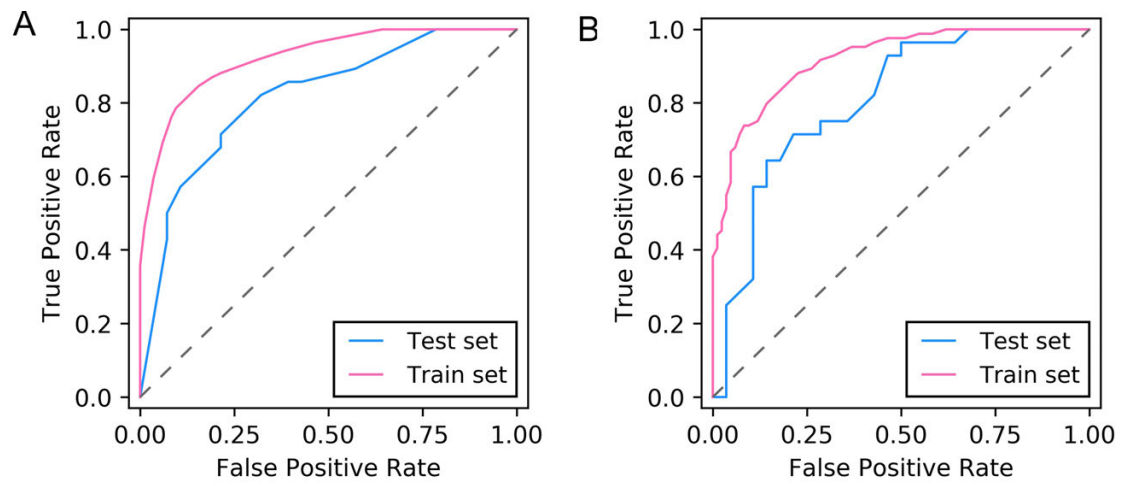


Fig. S18. ROC curve of the decision tree (A) and RuleFit (B) models trained on the fifth dataset split.

X[0]: Concentration (mg/L)
 X[1]: TEM size (nm)
 X[2]: Zeta potential (mV)

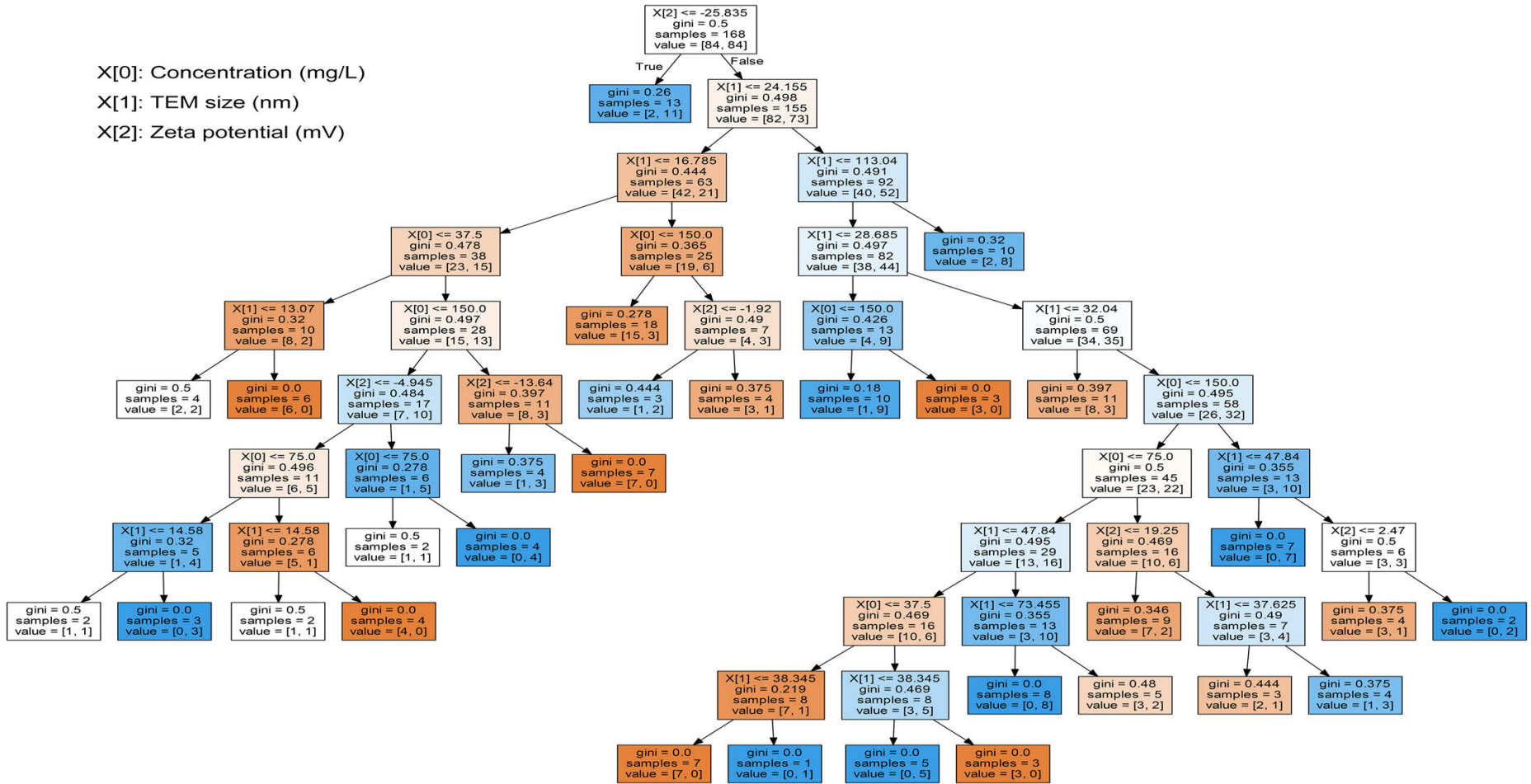


Fig. S19. The decision tree structure for root dry weight prediction based on three important features identified by post hoc interpretation of LightGBM models.

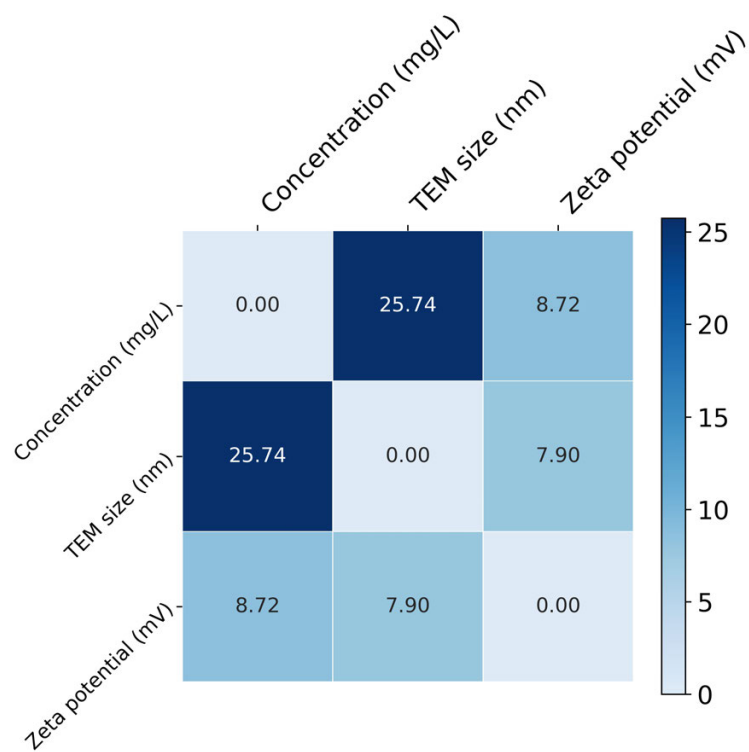


Fig. S20. SHAP interaction values of all features in the decision tree model.

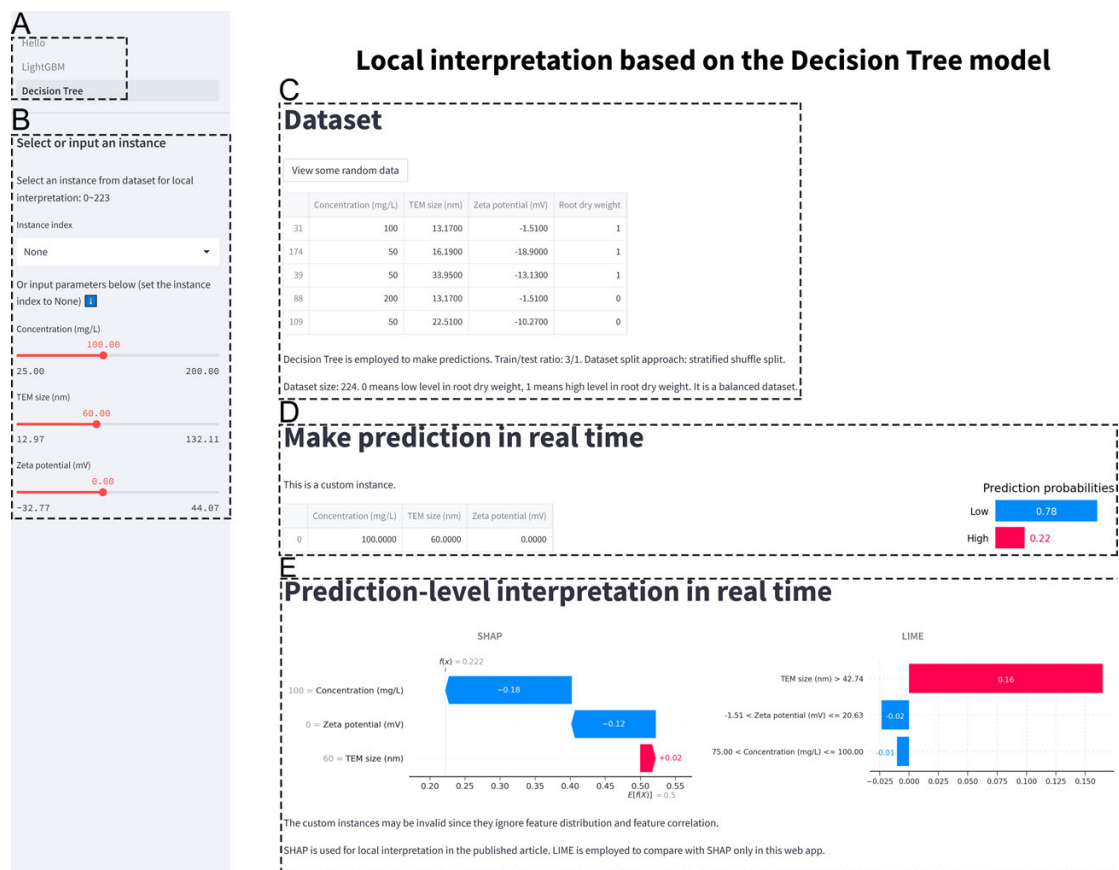


Fig. S21. The online interactive website for prediction-level interpretation (<https://seed-nanopriming-isar.streamlit.app/>). A, Navigation to different pages on this website. Hello: welcome page. LightGBM: local interpretation in the LightGBM model. Decision tree: local interpretation in the decision tree model. B, Select an instance from the used dataset or customize a sample. C, Dataset introduction and some random instances. D, Show the selected/custom instance and make a prediction. E, Prediction-level interpretation for this prediction.

Tables

Table S1.1. An overview of the used dataset and the prediction target (root dry weight).

| Feature/target | Percentage/range |
|--------------------------------------|-----------------------------------|
| Composition | |
| <i>SiO₂</i> | 14.29% |
| <i>CuO</i> | 14.29% |
| <i>CeO₂</i> | 14.29% |
| <i>Fe₃O₄</i> | 14.29% |
| <i>ZnO</i> | 14.29% |
| <i>TiO₂</i> | 14.29% |
| <i>α-Fe₂O₃</i> | 7.14% |
| <i>γ-Fe₂O₃</i> | 7.14% |
| Morphology | |
| <i>Compound</i> | 57.14% |
| <i>Spherical</i> | 42.86% |
| TEM size | 12.97~132.11 nm |
| TEM size SD | 2.65~32.82 nm |
| Concentration | 25, 50, 100, 200 mg/L |
| Hydrodynamic diameter | 197~933.73 nm |
| PdI | 0.17~0.81 |
| Zeta potential | -32.77~44.07 mV |
| BET surface area | 4.07~200.84 m ² /g |
| Target: Root dry weight | 1 for high level, 0 for low level |

Table S1.2. Detailed analysis of the numerical features collected in this study.

| | TEM size (nm) | TEM size SD (nm) | Concentra tion (mg/L) | Hydrodyn amic diameter (nm) | PdI | Zeta potential (mV) | BET surface area (m ² /g) |
|--------------|------------------|---------------------|-----------------------------|--------------------------------------|----------|---------------------------|---|
| count | 224 | 224 | 224 | 224 | 224 | 224 | 224 |
| mean | 39.19571 | 9.621429 | 93.75 | 459.0236 | 0.369286 | 3.439286 | 73.07857 |
| std | 32.9445 | 8.734165 | 67.17389 | 241.9576 | 0.215105 | 20.58079 | 60.58844 |
| min | 12.97 | 2.65 | 25 | 197 | 0.17 | -32.77 | 4.07 |
| 25% | 17.38 | 3.11 | 43.75 | 264.87 | 0.22 | -12.93 | 25.31 |
| 50% | 28.685 | 6.89 | 75 | 363.47 | 0.26 | 1.595 | 56.85 |
| 75% | 42.74 | 10.98 | 125 | 660 | 0.54 | 20.63 | 117.09 |
| max | 132.11 | 32.82 | 200 | 933.73 | 0.81 | 44.07 | 200.84 |

Table S2. The version of the main software and packages used in this study.

| Software/packages | Version |
|--------------------------|----------------|
| Python | 3.10.8 |
| scikit-learn | 1.1.2 |
| shap | 0.39.0 |
| PDPbox | 0.2.1 |
| imodels | 1.2.5 |
| lime | 0.2.0.1 |
| scipy | 1.7.3 |
| numpy | 1.21.5 |
| streamlit | 1.13.0 |
| R | 4.2.2 |
| agricolae | 1.3-5 |
| ropls | 1.30.0 |

Table S3. The determined model hyperparameters of LightGBM models.

| Random state | min_data_in_leaf | min_sum_hessian_in_leaf | max_bin | max_depth | num_leaves | learning_rate |
|--------------|------------------|-------------------------|---------|-----------|------------|---------------|
| 1 | 10 | 1 | 5 | 6 | 9 | 0.060 |
| 2 | 10 | 1 | 8 | 3 | 4 | 0.060 |
| 3 | 7 | 1 | 9 | 4 | 5 | 0.067 |
| 4 | 7 | 1 | 6 | 4 | 6 | 0.049 |
| 5 | 1 | 3 | 14 | 4 | 5 | 0.081 |
| 6 | 15 | 3 | 15 | 4 | 6 | 0.064 |
| 7 | 17 | 1 | 15 | 5 | 7 | 0.100 |
| 8 | 1 | 3 | 15 | 6 | 9 | 0.100 |
| 9 | 1 | 3 | 10 | 6 | 9 | 0.141 |
| 10 | 14 | 2 | 6 | 4 | 5 | 0.074 |

Table S4. Three group division of 56 nanopriming treatments based on the SRI under salinity stress.

| Group | Treatments (Composition: Size(nm) : Concentration(mg/L)) | Average SRI |
|-------------|---|-------------|
| High (7) | ZnO:30:200, CeO ₂ :<100:200, SiO ₂ :20:50, CeO ₂ :20-50:100, SiO ₂ :50:50, Fe ₃ O ₄ :50:100, Fe ₃ O ₄ :20:100 | 11.39 |
| Middle (16) | CeO ₂ :<100:50, α -Fe ₂ O ₃ :30:100, CuO:40:25, SiO ₂ :20:200, ZnO:50:200, SiO ₂ :50:100, SiO ₂ :50:200, α -Fe ₂ O ₃ :30:25, CeO ₂ :20-50:25, α -Fe ₂ O ₃ :30:200, ZnO:30:50, ZnO:50:50, CuO:40:50, CeO ₂ :20-50:50, ZnO:50:25, SiO ₂ :50:25, SiO ₂ :20:25, Fe ₃ O ₄ :50:200, CeO ₂ :<100:100, SiO ₂ :20:100, ZnO:30:25, CeO ₂ :20-50:200, CuO:40:200, Fe ₃ O ₄ :20:50, CuO:50-100:25, α -Fe ₂ O ₃ :30:50, Fe ₃ O ₄ :50:25, TiO ₂ :40:25, TiO ₂ :20:25, γ -Fe ₂ O ₃ :<50:100, CeO ₂ :<100:25, TiO ₂ :20:50, TiO ₂ :40:100, TiO ₂ :40:200, Fe ₃ O ₄ :20:200, CuO:40:100, γ -Fe ₂ O ₃ :<50:50, γ -Fe ₂ O ₃ :<50:25, TiO ₂ :20:200, CuO:50-100:50, CuO:50-100:200, ZnO:30:100, CuO:50-100:100, ZnO:50:100, TiO ₂ :40:50, Fe ₃ O ₄ :20:25, Fe ₃ O ₄ :50:50, γ -Fe ₂ O ₃ :<50:200, TiO ₂ :20:100 | 10.74 |
| Low (33) | | 9.99 |

Table S5. The 7-fold cross-validation results of established PLS-DA and OPLS-DA models.

| Ion mode | Type | R²X(cum) | R²Y(cum) | Q²(cum) | Treatments |
|-----------------|-------------|----------------------------|----------------------------|---------------------------|-------------------|
| positive | PLS-DA | 0.679 | 0.994 | 0.912 | SN_vs_SC |
| positive | OPLS-DA | 0.679 | 0.994 | 0.725 | SN_vs_SC |
| positive | PLS-DA | 0.85 | 0.99 | 0.895 | HdN_vs_HdC |
| positive | OPLS-DA | 0.85 | 0.99 | 0.85 | HdN_vs_HdC |
| negative | PLS-DA | 0.508 | 0.954 | 0.744 | SN_vs_SC |
| negative | OPLS-DA | 0.683 | 0.994 | 0.87 | SN_vs_SC |
| negative | PLS-DA | 0.769 | 0.978 | 0.773 | HdN_vs_HdC |
| negative | OPLS-DA | 0.769 | 0.978 | 0.899 | HdN_vs_HdC |

Table S6. The rules determined by the RuleFit algorithm.

| No. | Rule | Type | Coefficient | Support | Importance |
|-----|--|------|-------------|---------|------------|
| 39 | Concentration (mg/L) \leq 75.0 and Concentration (mg/L) $>$ 37.5 and Zeta potential (mV) \leq 5.565 | rule | 2.2548 | 0.1310 | 0.7607 |
| 3 | Concentration (mg/L) \leq 37.5 and TEM size (nm) \leq 38.345 and TEM size (nm) $>$ 28.685 | rule | -3.0894 | 0.0536 | 0.6956 |
| 24 | Concentration (mg/L) $>$ 150.0 and TEM size (nm) \leq 38.345 and Zeta potential (mV) \leq -9.325 | rule | 2.6014 | 0.0714 | 0.6700 |
| 4 | Concentration (mg/L) $>$ 150.0 and TEM size (nm) \leq 32.04 and Zeta potential (mV) $>$ -9.325 | rule | -2.2350 | 0.0952 | 0.6561 |
| 9 | Concentration (mg/L) \leq 75.0 and TEM size (nm) \leq 24.155 and Zeta potential (mV) $>$ -14.585 | rule | -1.7272 | 0.1488 | 0.6147 |
| 21 | Concentration (mg/L) \leq 37.5 and Zeta potential (mV) $>$ -13.03 | rule | 1.4855 | 0.1964 | 0.5902 |
| 34 | Concentration (mg/L) $>$ 150.0 and TEM size (nm) $>$ 32.04 | rule | 1.8115 | 0.0893 | 0.5166 |
| 25 | Concentration (mg/L) $>$ 37.5 and Zeta potential (mV) $>$ -9.325 | rule | 0.9328 | 0.4643 | 0.4652 |
| 27 | Concentration (mg/L) $>$ 75.0 and TEM size (nm) \leq 47.84 and TEM size (nm) $>$ 24.155 and Zeta potential (mV) \leq 26.17 and Zeta potential (mV) $>$ -25.835 | rule | 1.4086 | 0.1071 | 0.4357 |
| 19 | Concentration (mg/L) $>$ 37.5 and TEM size (nm) \leq 47.84 and Zeta potential (mV) \leq 26.17 and Zeta potential (mV) $>$ -25.835 | rule | -0.8501 | 0.4286 | 0.4207 |
| 32 | Concentration (mg/L) \leq 75.0 and TEM size (nm) $>$ 24.155 and Zeta potential (mV) \leq 11.285 | rule | 1.3193 | 0.1131 | 0.4178 |
| 8 | Concentration (mg/L) \leq 37.5 and TEM size (nm) $>$ 28.685 and Zeta potential (mV) $>$ -9.325 | rule | -1.6738 | 0.0655 | 0.4140 |
| 14 | Zeta potential (mV) \leq -9.325 and Zeta potential (mV) $>$ -25.835 | rule | -0.7219 | 0.3036 | 0.3319 |
| 18 | Concentration (mg/L) $>$ 37.5 and TEM size (nm) \leq 19.155 and TEM size (nm) $>$ 13.07 | rule | 0.8465 | 0.1786 | 0.3242 |
| 7 | Concentration (mg/L) \leq 37.5 and TEM size (nm) \leq 19.155 and TEM size (nm) $>$ 13.07 | rule | -1.3037 | 0.0595 | 0.3085 |
| 16 | Concentration (mg/L) $>$ 75.0 and TEM size (nm) \leq 24.155 and Zeta potential (mV) $>$ -14.585 | rule | 0.8025 | 0.1429 | 0.2808 |
| 17 | Concentration (mg/L) $>$ 75.0 and TEM size (nm) \leq 113.04 | rule | -0.5303 | 0.4702 | 0.2647 |
| 12 | Concentration (mg/L) $>$ 37.5 and TEM size (nm) \leq 32.04 and TEM size (nm) $>$ 16.785 and Zeta potential (mV) $>$ -25.835 | rule | -0.6072 | 0.2143 | 0.2491 |
| 11 | Concentration (mg/L) $>$ 75.0 and TEM size (nm) $>$ | rule | -0.7658 | 0.1012 | 0.2310 |

| | | | | | |
|----|--|------|---------|--------|--------|
| | 47.84 and Zeta potential (mV) > -25.835 | | | | |
| 6 | Concentration (mg/L) > 150.0 and TEM size (nm) <= 16.785 and Zeta potential (mV) > -13.64 | rule | -1.1142 | 0.0417 | 0.2226 |
| 10 | Concentration (mg/L) <= 75.0 and Concentration (mg/L) > 37.5 and TEM size (nm) <= 113.04 and TEM size (nm) > 38.345 | rule | -0.7300 | 0.0536 | 0.1644 |
| 37 | Concentration (mg/L) <= 150.0 and TEM size (nm) <= 28.685 and TEM size (nm) > 24.155 and Zeta potential (mV) > -25.835 | rule | 0.6808 | 0.0595 | 0.1611 |
| 29 | TEM size (nm) <= 21.72 and TEM size (nm) > 19.155 | rule | 0.5940 | 0.0774 | 0.1587 |
| 28 | Concentration (mg/L) <= 150.0 and TEM size (nm) <= 32.04 and TEM size (nm) > 16.785 and Zeta potential (mV) > 26.17 | rule | 0.6206 | 0.0595 | 0.1468 |
| 40 | Concentration (mg/L) > 37.5 and TEM size (nm) > 113.04 and Zeta potential (mV) <= 26.17 | rule | 0.5028 | 0.0476 | 0.1071 |
| 5 | Concentration (mg/L) <= 37.5 and Zeta potential (mV) <= -13.03 and Zeta potential (mV) > -25.835 | rule | -0.5116 | 0.0417 | 0.1022 |
| 15 | Concentration (mg/L) <= 37.5 and TEM size (nm) <= 113.04 | rule | 0.2161 | 0.2500 | 0.0936 |
| 26 | TEM size (nm) > 19.155 and Zeta potential (mV) <= -11.6 | rule | 0.1976 | 0.2262 | 0.0827 |
| 20 | TEM size (nm) > 21.72 and Zeta potential (mV) <= 26.17 | rule | -0.1366 | 0.4762 | 0.0682 |
| 22 | Zeta potential (mV) <= 26.17 and Zeta potential (mV) > -25.835 | rule | -0.1407 | 0.7798 | 0.0583 |
| 23 | TEM size (nm) <= 16.785 and Zeta potential (mV) <= 26.17 and Zeta potential (mV) > -25.835 | rule | -0.1050 | 0.2262 | 0.0439 |
| 30 | Concentration (mg/L) <= 75.0 and TEM size (nm) > 32.04 | rule | 0.0508 | 0.2024 | 0.0204 |
| 31 | Concentration (mg/L) > 37.5 and TEM size (nm) <= 32.04 and TEM size (nm) > 16.785 and Zeta potential (mV) <= -21.52 | rule | 0.0828 | 0.0536 | 0.0186 |
| 13 | TEM size (nm) <= 32.76 and Zeta potential (mV) <= 26.17 and Zeta potential (mV) > -25.835 | rule | -0.0362 | 0.4405 | 0.0180 |
| 38 | Zeta potential (mV) <= -25.835 | rule | 0.0327 | 0.0774 | 0.0087 |
| 35 | TEM size (nm) <= 113.04 and Zeta potential (mV) <= -25.835 | rule | 0.0296 | 0.0774 | 0.0079 |
| 33 | TEM size (nm) <= 38.345 and Zeta potential (mV) <= -25.835 | rule | 0.0158 | 0.0774 | 0.0042 |
| 36 | TEM size (nm) > 19.155 and Zeta potential (mV) <= -22.95 | rule | 0.0119 | 0.0774 | 0.0032 |